Observation of exceptional points in electronic circuits

T Stehmann, W D Heiss and F G Scholtz

Institute of Theoretical Physics, University of Stellenbosch, South Africa

Abstract
Two damped coupled oscillators have been used to demonstrate the occurrence
of exceptional points in a purely classical system. The implementation was
achieved with electronic circuits in the kHz-range. The experimental results
perfectly match the mathematical predictions at the exceptional point. A
discussion about the universal occurrence of exceptional points—connecting
dissipation with spatial orientation—concludes this paper.

PACS numbers: 03.65.Vf, 02.30.−f, 41.20.−q

A surprising phenomenon occurring in systems described by non-Hermitian Hamiltonians has
been observed in a number of experiments: the coalescence of two eigenmodes. If the system
depends on some interaction parameter λ, the value λ_{EP} at which the coalescence occurs
is called an exceptional point (EP) [1]. At an EP, the eigenvalues *and* eigenvectors show
branch point singularities [1–5] as functions of λ. This stands in sharp contrast to two-fold
degeneracies, where no singularity but rather a diabolic point [6] occurs. EPs have been
described in laser induced ionization of atoms [7], in acoustical systems [8], and have actually
been observed in microwave cavities [9–11], in optical properties of certain absorptive media
[12, 13] and in 'crystals of light' [14]. The broad variety of physical systems showing EPs
indicates that their occurrence is *generic*. So far EPs have been analysed for the special case of
a complex symmetric effective Hamiltonian [15] used for the description of dissipative wave
mechanical systems such as in microwave cavities.

The physical interest in EPs is not only due to their universal occurrence in virtually all
problems of matrix diagonalization. It is in particular the chiral character associated with
the wavefunctions at the EP [16]. This has been experimentally confirmed recently [11] and
also thoroughly discussed in optics for anisotropic absorptive media [17]. The fascinating
point is the wavefunction at the EP: not only is there—at the point of the two coalescing
energies—one and only one state vector, but—for a complex symmetric matrix—its form is

given by

$$|\psi_{\text{EP}}^{+}\rangle = \begin{pmatrix} 0 \\ \vdots \\ i \\ 1 \\ 0 \\ \vdots \end{pmatrix} \quad \text{or} \quad |\psi_{\text{EP}}^{-}\rangle = \begin{pmatrix} 0 \\ \vdots \\ -i \\ 1 \\ 0 \\ \vdots \end{pmatrix}. \tag{1}$$

Only one EP of the pair is accessible in the laboratory as only one is associated with a negative sign of the imaginary part of the energy. The labels of the non-vanishing components in equation (1) are the labels of the two coalescing energies. Note that there is no parameter dependence; the form of the state vector is robust. We may associate this form with a circularly polarized wave. For a general non-Hermitian matrix the ratio of the two relevant components is no longer $\pm i$ but an arbitrary complex number that can in general be associated with an elliptic polarisation [17].

In this paper we report the results of a plain classical experiment where an EP has been identified and so has the orientation that goes with it. It is the case of two coupled damped oscillators. This has been proposed in [18] for two mechanical oscillators. In the quoted paper a discussion of the EPs is extended to general matrices being no longer complex symmetric. In fact, the classical equations of motion for the momenta p_j and coordinates q_j read for the two mechanical oscillators

$$\frac{\mathrm{d}}{\mathrm{d}t} \begin{pmatrix} p_1 \\ p_2 \\ q_1 \\ q_2 \end{pmatrix} = \mathcal{M} \begin{pmatrix} p_1 \\ p_2 \\ q_1 \\ q_2 \end{pmatrix} + \begin{pmatrix} c_1 \\ c_2 \\ 0 \\ 0 \end{pmatrix} \exp(\mathrm{i}\omega t) \tag{2}$$

with

$$\mathcal{M} = \begin{pmatrix} -2g - 2k_1 & 2g & -f - \omega_1^2 & f \\ 2g & -2g - 2k_2 & f & -f - \omega_2^2 \\ 1 & 0 & 0 & 0 \\ 0 & 1 & 0 & 0 \end{pmatrix} \tag{3}$$

where $\omega_j - \mathrm{i}k_j$, $j = 1, 2$ are essentially the damped frequencies without coupling and f and g are the coupling spring constant and damping of the coupling, respectively. The driving force is assumed to be oscillatory with one single frequency and acting on each particle with amplitude c_j. Here we are interested only in the stationary solution being the solution of the inhomogeneous equation which reads

$$\begin{pmatrix} p_1 \\ p_2 \\ q_1 \\ q_2 \end{pmatrix} = (\mathrm{i}\omega - \mathcal{M})^{-1} \begin{pmatrix} c_1 \\ c_2 \\ 0 \\ 0 \end{pmatrix} \exp(\mathrm{i}\omega t). \tag{4}$$

Resonances occur for the real values ω of the complex solutions of the secular equation

$$\det|\mathrm{i}\omega - \mathcal{M}| = 0 \tag{5}$$

and EPs occur for the complex values ω where

$$\frac{\mathrm{d}}{\mathrm{d}\omega} \det|\mathrm{i}\omega - \mathcal{M}| = 0 \tag{6}$$

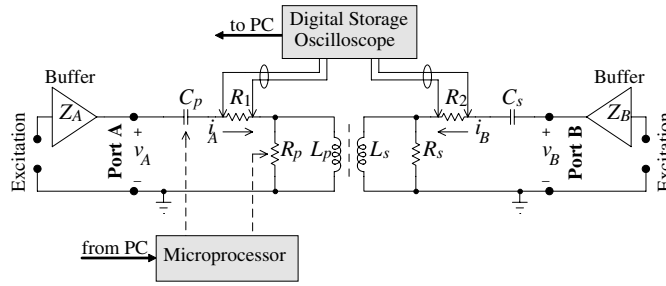is fulfilled together with equation (5). Note that $\mathcal{M}$ is non-symmetric.

Figure 1. Measurement set-up.

Table 1. Component values.

Component	Value	Unit	Tolerance (%)
C_p[a]	65	nF	5
R_1	3.0	Ω	10
R_p[b]	520	Ω	5
L_p	1.80	mH	5
L_s	2.55	mH	5
R_s	10.0	kΩ	5
R_2	3.0	Ω	10
C_s	47	nF	5
M	$0.14\sqrt{L_p L_s} = 0.3$	mH	5

[a] Can be varied from 39.0 to 77.6 nF in steps of 0.22 nF.
[b] Can be varied from 430 to 610 Ω in steps of 10 Ω.

For easy implementation electronic circuits are used rather than the mechanical oscillators. The momenta and coordinates are replaced by voltage and current, respectively. The unperturbed undamped frequencies are given by $\omega_j^2 = 1/(L_j C_j)$ with L and C being the inductance and capacitance, while damping and coupling are effected by resisters and mutual inductance. To allow for complex values of the effective inductance, resisters have been used in parallel to the inductance.

The actual experimental set-up is shown in figure 1. The two circuit parameters that can be changed are the circuit capacitance C_p and the parallel resistance R_p. Standard electronic components were used to construct the circuit. The component values are summarized in table 1. The two inductors consist of multi-layer cylindrical air core windings wound onto PVC plastic coil formers. The coils are placed next to each other with their geometric axes aligned. The distance between them can be varied in order to change the coupling, i.e. the mutual inductance of the two coils. Input voltage signals v_A and v_B are connected to ports A and B of the circuit and are used to excite the system. The circuit response is given by the input currents i_A and i_B into ports A and B, respectively. The two input currents can be determined by measuring the voltage drop over the series resistances R_1 and R_2. Using Ohm's Law the currents can be calculated.

The input ports A and B of the circuit have to be excited by ideal voltage sources. In a practical set-up the excitation voltage sources must have output impedances, Z_A and Z_B, that are much lower than the input impedances of the two circuit ports. The minimum input impedance of ports A and B are approximately R_1 and R_2, respectively. Buffers are used to reduce the signal impedance such that $Z_A \ll R_1$ and $Z_B \ll R_2$.

A microprocessor is used to enable automatic multiple data collection. The microprocessor interfaces to a PC and varies the values of two circuit components C_p and R_p. The input currents are measured with a digital oscilloscope. The oscilloscope is connected to the same PC as the microprocessor. The data from the oscilloscope are read directly into the PC where it is processed. The complete experiment is controlled with a software package called LabVIEW. A program written in LabVIEW is responsible for communicating with the microprocessor and the digital oscilloscope and processing the measurement data.

The first step in the measurement process is to determine the system eigenvalues. The eigenvalues can be determined from the system's frequency response, i.e. the system's spectrum. The frequency response $F_A(\omega)$ of the system at port A is given by [19]

$$F_A(\omega) = \frac{I_A(\omega)}{V_A(\omega)} = \frac{\sum_{i=0}^{M} a_i \omega^i}{\sum_{i=0}^{N} b_i \omega^i} \tag{7}$$

with $M \leqslant N$. Here $V_A(\omega)$ and $I_A(\omega)$ are the spectra of the applied voltage signal and the input current response at port A, respectively. A similar expression holds for the frequency response at port B. For the circuit in figure 1, it is $N = M = 4$. The resonance frequencies are the zeros of the denominator in equation (7).

The system's frequency response can be determined by either performing measurements in the frequency or time domain. Time domain measurements yield more accurate results compared to frequency domain measurements. For a time domain measurement the system is excited by a short voltage pulse. The resulting response of the input current at a port is the impulse response of the system for that port. The Fourier transform of the impulse response is equal to the system's frequency response. The frequency response depends on the measurement configuration, i.e. the port where the impulse response is measured and the relative amplitude of the excitation pulse at ports A and B. In equation (7) only the roots of the numerator are dependent on the measurement configuration. The roots of the denominator, i.e. the eigenvalues, are independent of different measurement configurations.

In a practical set-up it is not possible to generate infinitely short pulses. However, the pulse width t_p must be small compared to the response time of the system. A valid impulse response must obey

$$t_p \ll \frac{1}{\max(|\omega_i|)} \tag{8}$$

with $\max(|\omega_i|)$ the eigenvalue with the largest modulus.

For this experiment both ports A and B where excited by the same voltage pulse. The input current into port A was measured. Applying a Fourier transform to the measured impulse response current the frequency response of the system is obtained. By fitting equation (7) to the measured data the coefficients a_i and b_i can be determined and the resulting eigenvalues of the system calculated.

The measured eigenvalues for different values of R_p and C_p are plotted on the complex energy plane in figure 2. Only two of the four eigenvalues of the system are plotted for each R_p and C_p value pair. The other two eigenvalues are mirrored with respect to the imaginary axis. Three resistance values were used, $R_p = 430$, $R_p = 470$ and $R_p = 510$. For each resistance value the capacitance was changed from 57.0 nF to 72.0 nF in steps of 0.22 nF. The resulting locus of eigenvalues repels from a point in the energy plane, which is the singular point of the system. The direction of each locus for an increasing value of C_p is indicated in figure 2. We denote the value of the frequency at the singular point by S_1 and find $S_1 \approx 92\,000 - \mathrm{i}11\,500$ as indicated by a cross in figure 2. A second singular point S_2 (not shown) is also measured and
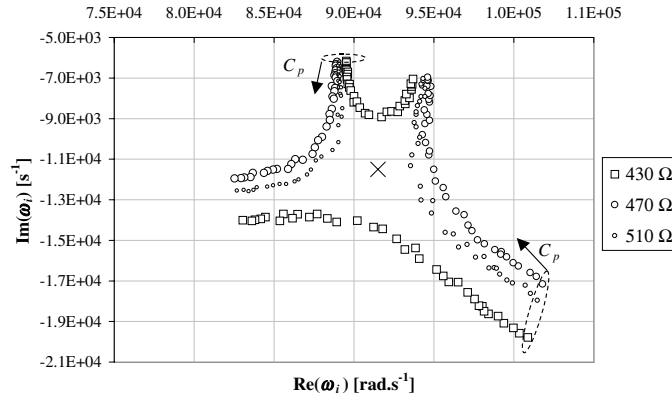
Figure 2. Measured system eigenvalues.

is mirrored with respect to the imaginary axis of the complex energy plane, i.e. $iS_1 = (iS_2)^*$. The measurement error is less than 6%.

In order to measure the system phase, the system has to be excited with a steady-state sinusoidal signal. A real sinusoidal signal always consists of two frequency components ω_1 and ω_2 for which $i\omega_1 = (i\omega_2)^*$. Hence, to measure the system phase at the singular point, the system is excited with two complex frequencies equal to the two singular point values S_1 and S_2. Furthermore, the circuit values of R_p and C_p are set to obtain eigenvalues as close as possible to the two singular points. The excitation signals at port A and B have the form

$$v(t) = C \sin(\omega_0 t + \phi_v) \, e^{-\gamma_0 t} \tag{9}$$

with $\omega_0 = |\mathrm{Re}(S_1)| = |\mathrm{Re}(S_2)|$ and $\gamma_0 = -\mathrm{Im}(S_1) = -\mathrm{Im}(S_2)$. The phase of the signal is ϕ_v and the amplitude C. For the measured system the value of γ_0 is positive ($\gamma \approx 11\,500\,\mathrm{s}^{-1}$). This implies a decaying sinusoidal signal.

The aim of the experiment is to measure the steady-state phase difference $\Delta\phi_i$ between the two input currents i_A and i_B. This is achieved by measuring the steady-state current response at the two ports simultaneously. The system is linear and the current response will have the same form as the excitation voltage in equation (9). The phase of the two input currents, ϕ_{iA} and ϕ_{iB}, can be extracted by fitting equation (9) to each of the measured current responses. The amplitude and phase are the fitting parameters. The phase difference is then simply $\Delta\phi_i = \phi_{iA} - \phi_{iB}$.

However, the signal in equation (9) is not a power signal, i.e. it does not have a finite power content. It is therefore not possible in practice to generate such a signal. To perform the phase measurement the excitation is switched on at $t = t_0$. For $t < t_0$ the signal is zero. The on-set of the signal at $t = t_0$ introduces a decaying transient response. A reliable measurement of the steady-state phase can only be performed at $t - t_0 \ll \gamma_0^{-1}$, where the transient response has decayed and can be neglected compared to the steady-state response.

To generate signals as described by equation (9) the circuit values of the circuit in figure 1 were so chosen that singular points and eigenvalues are obtained within the audible frequency range. This enables the excitation signals to be generated with a standard computer sound card. LabVIEW is again used to drive the sound card of the PC and generate any arbitrary signal within the audible frequency range (20 Hz to 20 kHz). The stereo output of a computer sound card can be used to generate two different signals simultaneously.
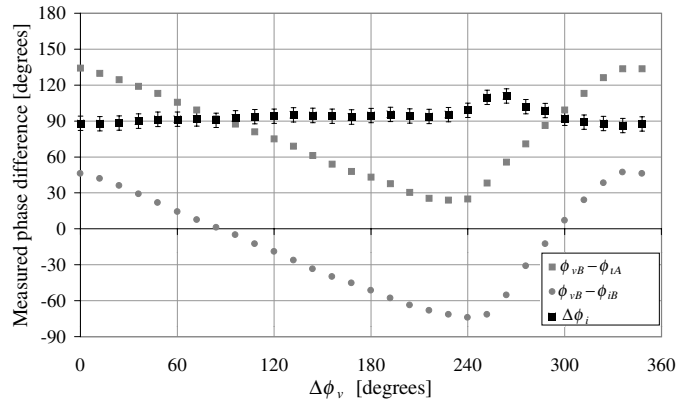
Figure 3. Measured system phase.

Finally, the steady-state phase difference $\Delta\phi_i$ between the input currents was measured while exciting both ports. The phase difference $\Delta\phi_v$ between the two excitation signals was varied from 0 to 2π radians. In figure 3 the measured current phase difference $\Delta\phi_i$ is plotted as a function of the excitation phase difference $\Delta\phi_v$. Also shown is the phase difference between the two input currents, i_A and i_B, and the excitation voltage v_B at port B. The measured phase difference $\Delta\phi_i$ is largely independent of the excitation phase difference $\Delta\phi_v$ with a value of approximately $\pi/2$ and a measurement error of 5%.

As far as the results are concerned we emphasize in particular two points: (i) the similarity of figure 2 with the corresponding figure for instance in [7] or [10] is striking; here it refers to electronic circuits, in the quoted papers to atomic physics or microwave cavities, respectively; (ii) the measured phase difference $\pi/2$ which is independent of the phase of the excitation, underlines once again the universal and robust chiral character of the state vector at the EP. We mention that, owing to the non-symmetric nature of the matrix considered (see equation (3)), there is in fact a slight deviation [18]. For the parameters chosen the precise quotient of the amplitudes actually is $-0.08 + i1.99\ldots$ and not i as in equation (1). In other words, there is a slight deviation from the circular towards an elliptic polarization. Yet an orientation prevails.

In this, like in all other experiments where EPs have been observed, dissipation is playing a foremost role. In fact, in quantum mechanics or optics, only absorption enables access in the laboratory to the singularity in the complex plane. And even in the experiment described in this paper, where the underlying matrices are no longer symmetric, dissipation is crucial to give rise to an EP. The decay of the states provides a direction of the time axis. In classical and quantum systems absorption—and decoherence in the latter case [20]—occurs due to the interaction with the environment, the presence of the open channels is effectively described by complex interaction parameters [15, 21] or, as in the present case, explicitly by Ohmic resisters.

In turn, the wavefunction at the EP is usually chiral in character as has been discussed in [16] and confirmed experimentally the first time in [11]. We see here an intrinsic connection— provided by the mathematics of an EP—between the direction of time and a given direction in space. In fact, the present experiment can serve to define a direction in one-dimensional space. At the EP, it is the one oscillator whose phase is leading while the phase of the other is lagging. These roles are fixed unequivocally for a given parameter set, unrelated to space. Viewing the oscillators placed along a straight line an orientation is defined along this line. This is not trivial and is caused by the mechanism at an EP: one, and only one-and-the-same

oscillator has the leading phase, and this feature is cast in stone by a system that has no *a priory* spatial orientation. It is dissipation that brings about spatial orientation.

This does not mean, at this stage, that a classical set-up can provide a distinction between left and right. One is tempted to find a truly three-dimensional setting where one EP might do just that.

Acknowledgments

References

[1] Kato T 1966 *Perturbation theory of linear operators* (Berlin: Springer)
[2] Heiss W D and Sannino A L 1990 *J. Phys. A: Math. Gen.* **23** 1167
    Heiss W D and Sannino A L 1991 *Phys. Rev.* A **43** 4159
[3] Berry M V and O'Dell D H J 1998 *J. Phys. A: Math. Gen.* **31** 2093
[4] Hernández E *et al* 2000 *J. Phys. A: Math. Gen.* **33** 4507
[5] Korsch H J and Mossmann S 2003 *J. Phys. A: Math. Gen.* **36** 2139
[6] Berry M V and Wilkinson M 1984 *Proc. R. Soc. Lond.* A **392** 15
[7] Latinne O *et al* 1995 *Phys. Rev. Lett.* **74** 46
[8] Shuvalov A L and Scott N H 2000 *Acta Mech.* **140** 1
[9] Brentano P v and Philipp M 1999 *Phys. Lett.* B **454** 171
    Philipp M *et al* 2000 *Phys. Rev.* E **62** 1922
[10] Dembowski C *et al* 2001 *Phys. Rev. Lett.* **86** 787
[11] Dembowski C *et al* 2003 *Phys. Rev. Lett.* **90** 034101
[12] Pancharatnam S 1955 *Proc. Ind. Acad. Sci.* **XLII** 86
[13] Berry M V 1994 *Curr. Sci.* **67** 220
[14] Oberthaler M K *et al* 1996 *Phys. Rev. Lett.* **77** 4980
[15] Heiss W D 1999 *Eur. Phys. J.* D **7** 1
    Heiss W D 2000 *Phys. Rev.* E **61** 929
[16] Heiss W D and Harney H L 2001 *Eur. Phys. J.* D **17** 149
    Harney H L and Heiss W D 2004 *Eur. Phys. J.* D **29** 429
[17] Berry M V and Dennis M R 2003 *Proc. Roy. Soc.* A **459** 1261
[18] Heiss W D 2004 *J. Phys. A: Math. Gen.* **37** 2455
[19] Nilsson J W and Riedel S A 1996 *Electric Circuits* (Reading, MA: Addision-Wesley)
[20] Leggett A J and Zurek W H 2002 in *Fundamentals of Quantum Information* ed W D Heiss LNP587 (Berlin: Springer)
[21] Mahaux C and Weidenmuller H A 1969 *Shell Model Approach to Nuclear Reactions* (Amsterdam: North-Holland)